Journal of Biomolecular NMR, **11:** 407–414, 1998.
KLUWER/ESCOM

NMR studies of *Borrelia burgdorferi* OspA, a 28 kDa protein containing a single-layer β-sheet

Thúy-Nga Pham & Shohei Koide*
Department of Biochemistry and Biophysics, University of Rochester Medical Center, Rochester, NY 14642, U.S.A.

Received 24 October 1997; Accepted 15 December 1997

Key words: Lyme disease, ^{15}N relaxation measurements, outer surface proteins, resonance assignments, β-sheet, triple resonance NMR spectroscopy

Abstract

The crystal structure of outer surface protein A (OspA) from *Borrelia burgdorferi* contains a single-layer β-sheet connecting the N- and C-terminal globular domains. The central β-sheet consists largely of polar amino acids and it is solvent-exposed on both faces, which so far appears to be unique among known protein structures. We have accomplished nearly complete backbone H, C and N and C^{β}/H^{β} assignments of OspA (28 kDa) using standard triple resonance techniques without perdeuteration. This was made possible by recording spectra at a high temperature (45 °C). The chemical shift index and ^{15}N T_1/T_2 ratios show that both the secondary structure and the global conformation of OspA in solution are similar to the crystal structure, suggesting that the unique central β-sheet is fairly rigid.

Introduction

Outer surface protein A (OspA) is an abundant immunogenic lipoprotein of the Lyme disease spirochete *Borrelia burgdorferi* with a molecular mass of 31 kDa (Barbour et al., 1983), and it is anchored to the membrane via a lipidated N-terminal cysteine (Brandt et al., 1990). Though little is known about the biological function of OspA, it has been demonstrated that antibodies directed against OspA can protect mice from *Borrelia burgdorferi* (Fikrig et al., 1990; Schaible et al., 1990). Vaccines based on OspA are in an advanced state of development (Johnson et al., 1995). A recombinant unlipidated form of OspA lacking the first 17 residues (28 kDa; referred to as OspA hereafter) is folded and soluble in aqueous solution (Dunn et al., 1990). Recently, the crystal structure of OspA complexed with the Fab fragment of a monoclonal antibody has been determined and refined to a resolution of 1.9 Å (Li et al., 1997). OspA has an extremely unusual structure (Figure 1): it is made of 21 consecutive antiparallel β-strands which are divided into four β-sheets and a single C-terminal α-helix; the molecule contains a nonglobular 'free-standing' β-sheet connecting globular N- and C-terminal domains (in this article, we term the three apparently distinct parts of the protein N-terminal domain (residues 17–105), central sheet (residues 106–141; strands 8–10) and C-terminal domain (residues 142–273), respectively, though we do not imply that these represent independent folding domains). The surface of the central β-sheet is largely exposed to the solvent on both faces (Figure 1). Such a solvent-exposed, single-layer β-sheet appears to be unique among known protein structures (Li et al., 1997). The most striking feature of the OspA structure is the lack of a hydrophobic core associated with the central β-sheet. Most antiparallel β-sheets observed in protein structures are amphipathic, and the hydrophobic face of such amphipathic β-sheets is usually buried in the interior to partially constitute a hydrophobic core.

In this work we ask whether the solution structure of OspA is similar to the crystal structure. The crystal structure of OspA suggests that the single-layer β-sheet, though never found before in natural proteins, is an energetically favorable conformation of

* To whom correspondence should be addressed.

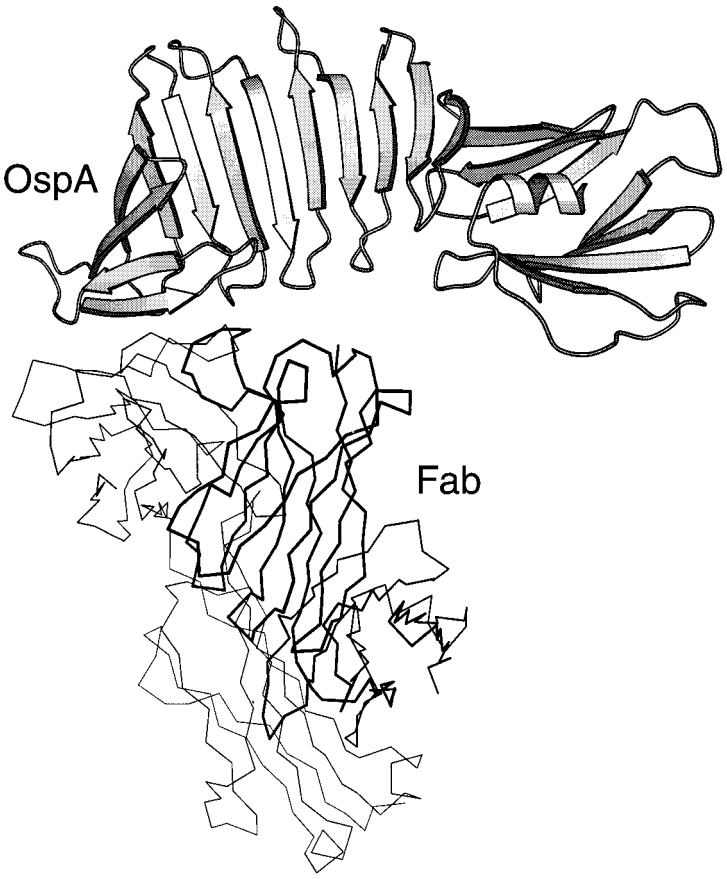

Figure 1. Schematic representation of secondary structure elements of the OspA-Fab crystal structure (Li et al., 1997). The locations of secondary structure elements were identified using the program PROMOTIF (Hutchinson and Thornton, 1996). The Fab fragment is shown as line drawing with the heavy chain as thicker lines. The figure was made with MOLSCRIPT (Kraulis, 1991).

polypeptides. However, one might expect that the central β-sheet is only marginally stable in solution but stabilized in the crystal structure due to antibody binding and/or lattice packing. For example, the central α-helix of calmodulin is flexible in solution, though the crystal structure shows a well-formed, apparently rigid α-helix (Barbato et al., 1992; Crivici and Ikura, 1995).

In order to characterize the solution conformation of OspA, we undertook NMR studies of OspA. The size of OspA (28 kDa) is close to those of the largest monomeric proteins for which complete backbone assignments have been reported (for a review, see Kay and Gardner, 1997). Here, we report the complete backbone resonance assignments and analyses of the secondary structure and the global conformation of OspA.

Materials and Methods

Sample preparation

The truncated form of OspA (residues 18–273 of full-length OspA plus an N-terminal Ala) was overexpressed in *Escherichia coli* BL21 (DE3) pLysS (Novagen) containing the T7 expression vector pET9-OspA (Dunn et al., 1990). Cells were grown in the M9 minimal medium (Sambrook et al., 1989) supplemented with ^{15}N NH_4Cl and/or ^{13}C glucose, and protein expression was induced by addition of isopropylthio-β-galactoside.

^{15}N-labeled OspA was purified from *E. coli* cell pellet to homogeneity by an SP-Sepharose FastFlow (Pharmacia) column with a sodium chloride gradient in sodium acetate buffer (10 mM, pH 4.6). From a single overexpression culture, $^{13}C/^{15}N$-labeled OspA was purified from the culture medium because a majority of the protein was released to the medium,

though the expression system is not designed to secrete OspA (Dunn et al., 1990). The cause of the leakage is unknown, but we suspect that T7 lysozyme coded for by the pLysS plasmid may have partially lysed the cells during growth. The pH of the medium was adjusted to 4.6 with concentrated acetate, and the protein was purified using an SP-Sepharose Fast-Flow column as described above. We found no significant differences in the ^{1}H,^{15}N-HSQC spectra of ^{15}N-OspA and $^{13}C/^{15}N$-OspA (data not shown), indicating that the proteins prepared from the cell pellet and the medium are indistinguishable in both chemical composition and solution conformation. NMR samples were dissolved in sodium phosphate buffer (10 mM, pH 6.0 at room temperature) containing sodium chloride (50 mM), EDTA (50 μM) and sodium azide (0.02%) in 95% H_2O/5% D_2O using an Amicon ultrafiltration cell.

NMR spectroscopy

All experiments were carried out on a Varian Unity INOVA 600 spectrometer using a 5 mm triple resonance probe with self-shielded pulsed field gradient (PFG). ^{1}H,^{15}N-HSQC, CBCA(CO)NH, HNCACB, C(CO)NH, HBHA(CO)NH and HNCO were recorded in standard manners (Bax and Grzesiek, 1993; Kay, 1995), including sensitivity enhancement (Palmer et al., 1991), PFG (Kay et al., 1992) and minimized water perturbation (Grzesiek and Bax, 1993b) whenever applicable. These three-dimensional triple resonance spectra were collected on a 1.5 mM solution of $^{13}C/^{15}N$-labeled OspA at 45 °C (the probe temperature was calibrated using ethyleneglycol). Experimental parameters are summarized in Table 1. NMR data were processed using the NMRPipe software (Delaglio et al., 1995) and analyzed using the NMRView software (Johnson and Blevins, 1994) on UNIX workstations. Linear prediction was applied in the ^{15}N dimension of the 3D experiments to extend the number of data points to 128. The chemical shifts have been deposited in the BioMagRes Bank (accession number 4076).

^{15}N Dynamics measurements

^{1}H-^{15}N NOE and ^{15}N T_1 and T_2 were measured on a 1.0 mM solution of ^{15}N-labeled OspA at 45 °C using published procedures (Farrow et al., 1994). The T_1 relaxation decay was sampled at 9 different time points (11, 55, 111, 222, 389, 555, 833, 1110 and 1943 ms) and the T_2 decay was sampled at 0, 16.6, 33.3, 66.6, 99.8 and 131.2 ms. T_1 and T_2 relaxation times were determined by nonlinear least-squares fitting of an exponential function. Errors in peak height measurements in individual spectra were estimated from noise in the baseplane, and errors associated with T_1 and T_2 values were then estimated by Monte Carlo simulation.

The NH bond vectors were calculated from an energy minimized structural model based on the OspA crystal structure. The program X-PLOR (Brünger, 1992) was used to add hydrogen atoms to the crystal structure coordinates (PDB entry code 1OSP) and to perform energy minimization using the CHARMM22 parameters. The inertia tensor was estimated from the crystal structure using the program PDBINERTIA (A.G. Palmer III, Columbia University). The theoretical dependence of T_1/T_2 ratios versus θ for an axially symmetric diffusion model (Lee et al., 1997) was used to fit the experimental data:

$$\begin{aligned} T_1/T_2 = {} & \{4J(0) + J(\omega_N - \omega_H) + 3J(\omega_N) \\ & + 6J(\omega_H) + 6J(\omega_N + \omega_H) \\ & + (q_{CSA}/3q_{DD})[4J(0) + 3J(\omega_N)]/ \\ & (\{2J(\omega_N - \omega_H) + 6J(\omega_N) + 12J(\omega_N + \omega_H) \\ & + (2(q_{CSA}/q_{DD})J(\omega_N)\} \end{aligned}$$

where $q_{DD} = 0.1(\mu_0/4\pi)^2(h/2\pi)^2\gamma_N^2\gamma_H^2 r_{NH}^{-6}$; $q_{CSA} = (2/15)\omega_N^2\Delta\sigma^2$; the spectral density function $J(\omega) = \sum_{j=1}^{3} A_j\tau_j/(1+\omega^2\tau_j^2)$ where $\tau_1^{-1} = 6D_\perp$, $\tau_2^{-1} = 5D_\perp + D_{||}$, $\tau_3^{-1} = 2D_\perp + 4D_{||}$, $A_1 = (3\cos^2\theta - 1)^2/4$, $A_2 = 3\sin^2\theta\cos^2\theta$, $A_3 = 0.75\sin^4\theta$; μ_0 is the permeability of free space; h is Planck's constant; ω_N and ω_H are the Larmor frequencies of the ^{15}N and ^{1}H spins, respectively; γ_N and γ_H are the gyromagnetic ratios of the ^{15}N and ^{1}H spins, respectively; r_{NH} is the internuclear N-H distance; $\Delta\sigma$ is the chemical shift anisotropy of the ^{15}N spin; $D_\perp$ and $D_{||}$ are two unique diffusion coefficients perpendicular and parallel to the unique axis of the diffusion tensor, respectively.

Results and Discussion

Resonance assignments

First, we have confirmed that OspA exists predominantly in the monomeric state in solution at 1.5 mM under the NMR conditions by measuring the diffusion rate (Altieri et al., 1995), and at a lower concentration by gel-filtration chromatography (data not shown). In

Table 1. Parameters for 3D experiments used in this study

Parameter	HNCO	CBCACONH	HNCACB	CCONH	HBHACONH
F_1 (Hz)	1660	9054	9054	9054	4200
F_2 (Hz)	2068	2068	2068	2068	2068
F_3 (Hz)	9001	9001	9001	9001	9001
t_1 (points*)	64	60	86	64	64
t_2 (points*)	47	50	50	51	50
t_3 (points*)	480	512	512	512	512
Total time (hr)	60	63	90	106	66

* In complex points.

addition, no concentration dependence has been observed in ^{1}H,^{15}N-HSQC spectra (data not shown), consistent with OspA being monomeric under the conditions used. The ^{1}H,^{15}N-HSQC spectrum of OspA (Figure 2a) shows an excellent spectral dispersion that is characteristic of a predominantly β-sheet protein.

Complete NMR assignments for the backbone ^{1}HN, ^{13}C and ^{15}N nuclei (except for those of the first and second residues due to rapid exchange with solvent, and the C′ resonance of Leu34 which precedes the single Pro residue) and the $^{13}C^{\beta}$ nuclei were obtained using a set of standard triple resonance experiments on $^{13}C/^{15}N$-labeled OspA. In addition, $^{1}H^{\alpha}$ and $^{1}H^{\beta}$ resonances for all but 14 residues have been assigned. Representative planes from triple resonance spectra are shown in Figure 2. We used the HNCO spectrum as the reference for bookkeeping. Initially, approximately 70% of the HNCO peaks could be assigned solely based on the CBCA(CO)NH and HNCACB spectra using the standard assignment procedures (Grzesiek and Bax, 1993a; Wittekind and Mueller, 1993). The correlation between the amide ^{1}H and ^{15}N pair to the intraresidue C^{β} resonance, which is critical for resonance assignment, was observed for all residues (except for Gly residues) in the HNCACB experiment, indicating that the size limit of the experiment is beyond 28 kDa at the temperature used (45 °C). The additional C(CO)NH spectrum allowed us to resolve ambiguities, leading to the complete backbone assignments. It should be noted that, despite the large size of OspA (28 kDa), perdeuteration was unnecessary to achieve the assignments. This is mainly because of the high stability of OspA which has permitted data collection at 45 °C, and an excellent spectral dispersion in the ^{1}H,^{15}N-HSQC spectrum. No changes were found in the HSQC spectrum recorded after all the 3D spectra were obtained, as compared to the spectrum of a freshly prepared sample, indicating that no significant changes occurred in the chemical and spatial structure of OspA over the course of the data collection. Our success indicates that these standard triple resonance experiments are applicable to a protein of this size (28 kDa) if spectra can be recorded at a relatively high temperature. Although data collection at a high temperature is of course limited by the thermal stability of a sample, it may be more readily applicable to larger proteins: a significant number of monomeric proteins are of similar size and whole proteins, in contrast to fragments, tend to possess higher thermal stabilities.

Secondary structure analysis

Locations of regular secondary structure elements in OspA in the solution state were analyzed using the chemical shift index (CSI) method (Wishart and Sykes, 1994). The deviations of the chemical shifts of ^{13}CO, $^{13}C^{\alpha}$ and $^{13}C^{\beta}$ nuclei from their respective random coil values are sensitive indicators of secondary structure, and the CSI method has been shown to accurately locate α-helices and β-strands (Wishart and Sykes, 1994). The results (Figure 3) suggest that all the β-strands, including those in the central β-sheet, and the single α-helix which have been identified in the crystal structure exist in the solution state, though this chemical shift analysis does not provide information on the global fold.

^{15}N relaxation measurements

The conformational dynamics of individual amide ^{1}H-^{15}N bond vectors were probed by measuring ^{1}H-^{15}N nuclear Overhauser effects (NOE). Residues in OspA which show reduced ^{1}H-^{15}N NOE are limited to those in the unstructured N-terminus and those in loops (Figure 4). Residues in the β-strands of the central β-sheet have ^{1}H-^{15}N NOEs close to the average, indicating

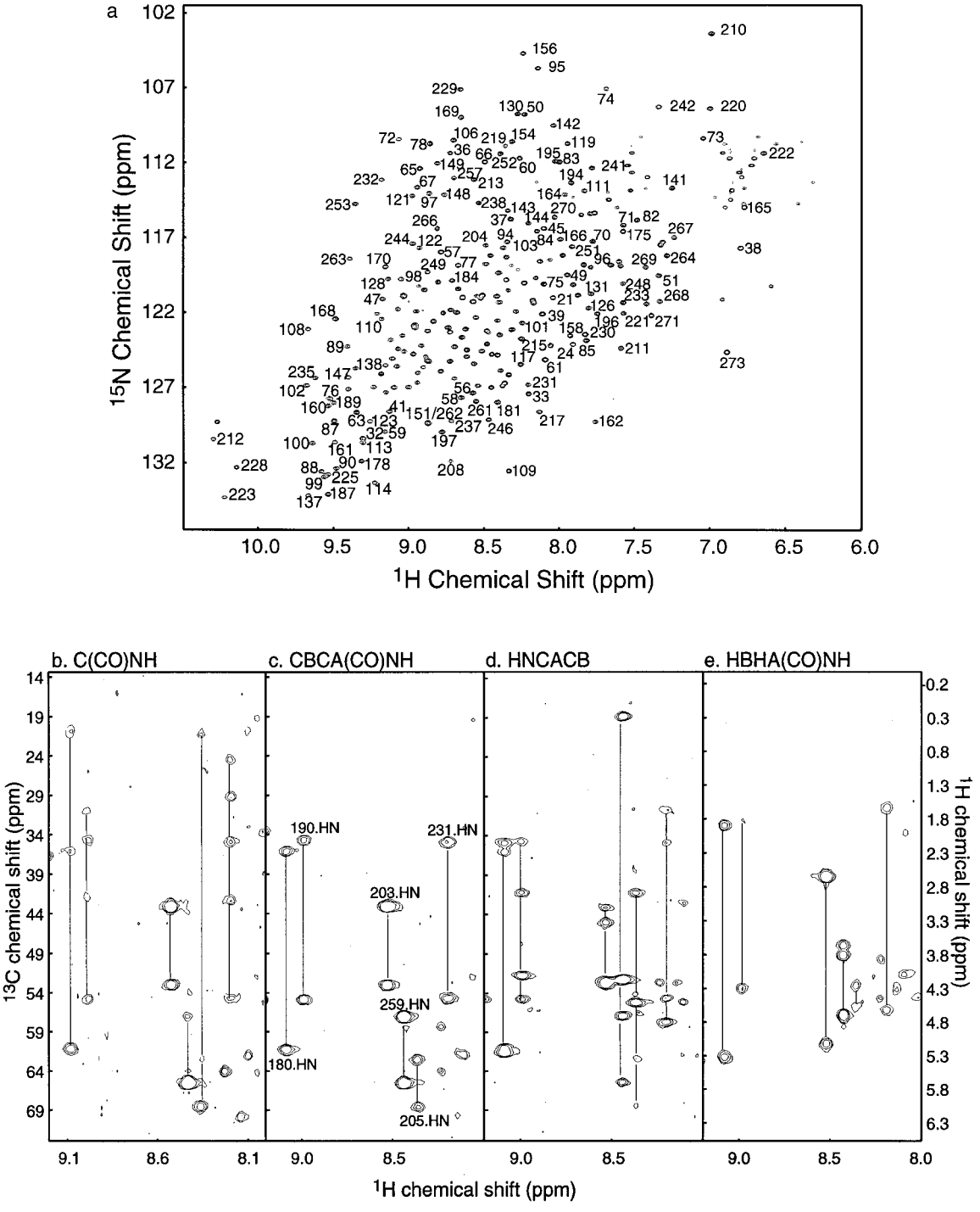

Figure 2. (a) ^{1}H,^{15}N-HSQC spectrum of OspA. The spectrum was recorded at 45 °C in approximately 1 h. Resonance assignments are indicated with residue numbers. Cross peaks in the central region of the spectrum are not labeled for clarity. The cross peak for Val199 is at ^{1}H= 3.98 ppm and ^{15}N= 120.77 ppm which lies outside the plot. (b–e) Planes at ^{15}N= 126.9 ppm of the C(CO)NH (b), CBCA(CO)NH (c), HNCACB (d) and HBHA(CO)NH (e) spectra of OspA. Assignments for the ^{1}HN shifts are indicated with residue numbers.

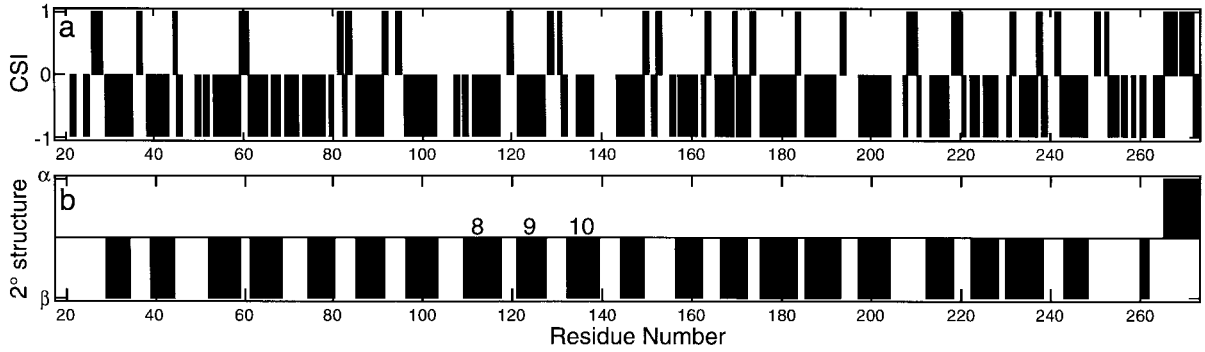

Figure 3. (a) The consensus chemical shift index (CSI) from $^{13}C^{\alpha}$, $^{13}C^{\beta}$ and ^{13}CO secondary chemical shifts determined according to a 'majority rules' algorithm (Wishart and Sykes, 1994). A minimum of three consecutive '−1's' suggests a β-strand, and a minimum of four '1's' suggests an α-helix. (b) Positions of β-strands (shown as negative bars) and an α-helix (shown as a positive bar) in the crystal structure.

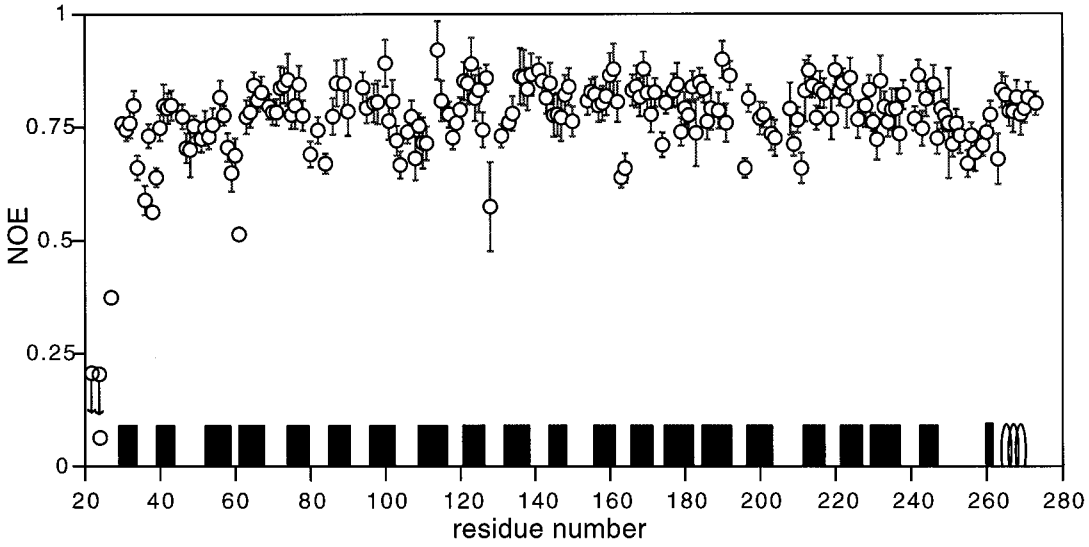

Figure 4. ^{1}H-^{15}N NOE intensities plotted versus residue number. Errors were estimated from the standard deviations of noise on the base plane. Residues 21 and 22 have values of −0.85 and −0.55, respectively, which fall outside the graph. The locations of β-strands (shown as bars) and an α-helix (shown as a coil) are also indicated.

that the central β-sheet is not highly mobile on a ps–ns time scale.

The global shape of OspA in solution was then probed by measuring the ^{15}N T_1/T_2 ratios. The ^{15}N T_1/T_2 ratio is a good measure for the rate at which each NH bond vector reorients due to global tumbling (Kay et al., 1989), and it can be used to define long-range order in a protein with a significant rotational diffusion anisotropy (Barbato et al., 1992; Tjandra et al., 1997). The crystal structure of OspA is highly elongated (Figure 1), and thus, if the solution conformation of OspA is similar, one should observe a large rotational diffusion anisotropy. The principal moments of the inertia tensor were calculated from the crystal structure (with no hydration shells) to be 0.21:0.90:1.00, indicating that it is reasonable to choose the axially symmetric diffusion model for a preliminary analysis described in this article. We have determined ^{15}N T_1 and T_2 relaxation times for 196 residues. Residues which showed large-amplitude internal motions (as judged by ^{1}H-^{15}N NOE < 0.65; residues 21, 22, 24, 27, 36, 38, 39, 59, 61, 128, 163) were excluded from further analysis. These residues are located in the unstructured N-terminal tail and in turns. An additional 15 residues (residues 89, 100, 102, 114, 123, 124, 126, 134, 136, 137, 145, 167, 169, 250, 270) exhibiting significantly reduced T_2 values had been excluded according to the criterion

of Tjandra et al. (1996; also see below). The final dataset consisting of the T_1/T_2 ratios for 170 residues gave a $(T_1/T_2)_{max}$ /$(T_1/T_2)_{min}$ ratio of 3.41, which clearly indicates a large rotational diffusion anisotropy of the molecule. Figure 5 shows the dependence of the ^{15}N T_1/T_2 ratios on the angle θ between the NH bond vectors and the unique axis of the diffusion tensor estimated from the crystal structure. Small T_1/T_2 ratios are clustered around $\theta = 90°$, while large T_1/T_2 ratios are dominantly found near $\theta = 0°$ and 180°. These data are consistent with an assumption that the unique axis of the diffusion tensor is parallel to that of the inertia tensor, i.e. the solution and the crystal structures of OspA are globally similar. Curve fitting of the equation describing the theoretical dependence of the ^{15}N T_1/T_2 ratios on the angle θ (Tjandra et al., 1995, 1997; Lee et al., 1997) to all data points (Figure 5) yielded a ratio of the two unique diffusion coefficients perpendicular and parallel to the assumed unique axis of the diffusion tensor ($D_\perp/D_\parallel$) of 0.57 ($\pm$ 0.03) and an effective overall correlation time ($\tau_{c,eff} = (2D_\parallel + 4D_\perp)^{-1}$, of 12.1 ns. In this analysis, the unique axis of the diffusion tensor was fixed parallel to that of the inertia tensor estimated from the crystal structure and its orientation was not optimized. Independent curve fitting to the data for the three segments gave $D_\perp/D_\parallel$ ratios of 0.54 ($\pm$0.04), 0.55 ($\pm$0.06) and 0.60 ($\pm$0.04) for the N-terminal, central and C-terminal domains, respectively, clearly indicating that the three segments tumble together as a fairly rigid entity. It should also be noted that 13 of the 15 residues which had been excluded from the analysis due to shorter T_2 times (see above) have the angle θ smaller than 30° (or larger than 150°), suggesting that their reduced T_2 relaxation times may be due to genuinely long correlation times (instead of due to chemical exchange broadening). Further experiments are planned to address this issue.

The chemical shift and relaxation analyses strongly suggest that the solution conformation of OspA is in fact similar to that observed in the crystal. It is surprising that the whole molecule is highly rigid and that the central single-layer β-sheet, which lacks a hydrophobic core, does not appear to be involved in large conformational movements such as bending and stretching. The central β-sheet contains characteristic cross-strand arrays of alternating Glu and Lys residues (Li et al., 1997). Such 'charge arrays' may be important for the rigidity of the central β-sheet. Further experiments, e.g. amide H-D exchange and site-directed mutagenesis, are planned to characterize the conformational stability of the central β-sheet and to elucidate the mechanism for stabilization of the unique single-layer β-sheet.

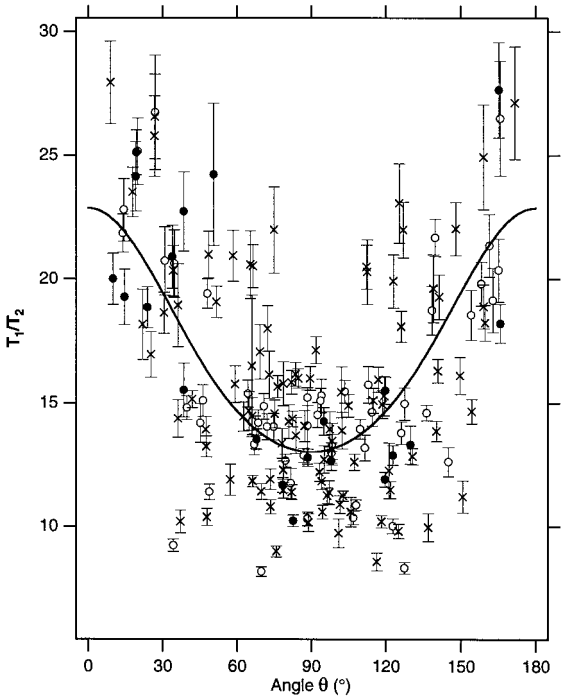

Figure 5. ^{15}N T_1/T_2 ratios plotted versus the angle θ between the NH bond vectors and the unique axis of the inertia tensor estimated from the crystal structure. Open circles show data for residues in the N-terminal domain, filled circles for residues in the central β-sheet and crosses for residues in the C-terminal domain.

Concluding remarks

We have achieved complete backbone assignments of OspA which is one of the largest monomeric proteins for which complete backbone assignments have so far been reported. We have shown that the solution conformation of OspA is similar to the crystal structure, and that the single-layer β-sheet is fairly rigid. The NMR assignments provide the foundation for further investigations of the folding and stability of the unique single-layer β-sheet and for mapping of OspA epitopes toward protective antibodies.

Acknowledgements

We thank Dr. J.J. Dunn for the OspA expression vector, Dr. C.L. Lawson for the crystal structure coordinates prior to publication and many helpful discussions, Dr. L.E. Kay for NMR pulse programs,

Dr. F. Delaglio for NMRPipe, Dr. B.A. Johnson for NMRView, Dr. A.G. Palmer, III for programs for analyzing ^{15}N dynamics data, and Dr. S.D. Kennedy and A. Koide for technical assistance. We thank Drs. R. Brüschweiler, N.A. Farrow and S.M. Pascal for helpful discussions.

References

Altieri, A.S., Hinton, D.P. and Byrd, R.A. (1995) *J. Am. Chem. Soc.*, **117**, 7566–7567.

Barbato, G., Ikura, M., Kay, L.E., Pastor, R.W. and Bax, A. (1992) *Biochemistry*, **31**, 5269–5278.

Barbour, A.G., Tessier, S.L. and Todd, W.J. (1983) *Infect. Immun.*, **41**, 795–804.

Bax, A. and Grzesiek, S. (1993) *Acc. Chem. Res.*, **26**, 131–138.

Brandt, M.E., Riley, B.S., Radolf, J.D. and Norgard, M.V. (1990) *Infect. Immun.*, **58**, 983–991.

Brünger, A.T. (1992) X-PLOR (Version 3.1): *A system for X-ray crystallography and NMR*, Yale University Press, New Haven, CT.

Crivici, A. and Ikura, M. (1995) Annu. Rev. Biophys. Biomol. Struct., **24**, 85–116.

Delaglio, F., Grzesiek, S., Vuister, G.W., Zhu, G., Pfeifer, J. and Bax, A. (1995) *J. Biomol. NMR*, **6**, 277–293.

Dunn, J.J., Lade, B.N. and Barbour, A.G. (1990) *Protein Expr. Purif.*, **1**, 159–168.

Farrow, N.A., Muhandiram, R., Singer, A.U., Pascal, S.M., Kay, C.M., Gish, G., Shoelson, S.E., Pawson, T., Forman-Kay, J.D. and Kay, L.E. (1994) *Biochemistry*, **33**, 5984–6003.

Fikrig, E., Barthold, S.W., Kantor, F.S. and Flavell, R.A. (1990) *Science*, **250**, 553–6.

Grzesiek, S. and Bax, A. (1993a) *J. Biomol. NMR*, **3**, 185–204.

Grzesiek, S. and Bax, A. (1993b) *J. Am. Chem. Soc.*, **115**, 12593–12594.

Hutchinson, E.G. and Thornton, J.M. (1996) *Protein Sci.*, **5**, 212–220.

Johnson, B.A. and Blevins, R.A. (1994) *J. Biomol. NMR*, **4**, 603–614.

Johnson, B.J.B., Sviat, S.L., Happ, C.M., Dunn, J.J., Frantz, J.C., Mayer, L.W. and Piesman, J. (1995) *Vaccine*, **13**, 1086–1094.

Kay, L.E. (1995) *Curr. Opin. Struct. Biol.*, **5**, 674–681.

Kay, L.E. and Gardner, K.H. (1997) *Curr. Opin. Struct. Biol.*, **7**, 722–731.

Kay, L.E., Keifer, P. and Saarinen, T. (1992) *J. Am. Chem. Soc.*, **114**, 10663–10665.

Kay, L.E., Torchia, D.A. and Bax, A. (1989) *Biochemistry*, **28**, 8972–8979.

Kraulis, P. (1991) *J. Appl. Crystallogr.*, **24**, 946–950.

Lee, L.K., Rance, M., Chazin, W.J. and Palmer, A.G. (1997) *J. Biomol. NMR*, **9**, 287–298.

Li, H., Dunn, J.J., Luft, B.J. and Lawson, C.L. (1997) *Proc. Natl. Acad. Sci. USA*, **94**, 3584–3589.

Palmer, A.G., Cavanagh, J., Wright, P.E. and Rance, M. (1991) *J. Magn. Reson.*, **93**, 151–170.

Sambrook, J., Fritsch, E.F. and Maniatis, T. (1989) *Molecular Cloning: A Laboratory Manual*, 2nd ed., Cold Spring Harbor Laboratory Press, Cold Spring Harbor, NY.

Schaible, U.E., Kramer, M.D., Eichmann, K., Modolell, M., Museteanu, C. and Simon, M.M. (1990) *Proc. Natl. Acad. Sci. USA*, **87**, 3768–3772.

Tjandra, N., Feller, S.E., Pastor, R.W. and Bax, A. (1995) *J. Am. Chem. Soc.*, **117**, 12562–12566.

Tjandra, N., Garrett, D.S., Gronenborm, A.M., Bax, A. and Clore, G.M. (1997) *Nat. Struct. Biol.*, **4**, 443–449.

Tjandra, N., Wingfield, P., Stahl, S. and Bax, A. (1996) *J. Biomol. NMR*, **8**, 273–284.

Wishart, D.S. and Sykes, B.D. (1994) *J. Biomol. NMR*, **4**, 171–180.

Wittekind, M. and Mueller, L. (1993) *J. Magn. Reson.*, **B101**, 201–205.